JACS
JOURNAL OF THE AMERICAN CHEMICAL SOCIETY

Communication

pubs.acs.org/JACS

Fabrication of *c*-Axis Oriented ZSM-5 Hollow Fibers Based on an in Situ Solid−Solid Transformation Mechanism

Kui Shen, Weizhong Qian,* Ning Wang, Chang Su, and Fei Wei

Beijing Key Laboratory of Green Chemical Reaction Engineering and Technology, Department of Chemical Engineering, Tsinghua University, Beijing 100084, P.R. China

Supporting Information

ABSTRACT: We report, for the first time, the preparation of novel *c*-axis oriented ZSM-5 hollow fibers by a combination of seeding and steam-assisted crystallization method using quartz fibers as the temporary soft substrate and Si source. The growth of such unique structure undergoes the development of a *b*-axis oriented ZSM-5 cylinder, followed by the growth of *c*-axis oriented ZSM-5 crystals vertically inside the cylinder and then outside the cylinder, by an in situ solid−solid transformation mechanism. The obtained ZSM-5 hollow fibers are composed of pure hierarchical ZSM-5 crystals with high crystallinity, good structural stability, and high surface area and have potential applications for microreactors, separators, and catalysts. The catalytic performance of ZSM-5 hollow fibers is tested in the methanol to gasoline reaction, as an example of their practical application. They exhibit both higher yield of gasoline and far longer lifetime compared to the conventional ZSM-5 due to the improved mass and heat diffusion rate inside the meso-/macropores of *c*-axis oriented structure.

As one of the most important commercial zeolites, ZSM-5 has high specific surface area, tunable acidity, excellent ion-exchange ability, high hydrothermal stability, and excellent shape selectivity and finds wide application in industrial applications.[1] Common textures of the ZSM-5 based catalyst used in fixed bed reactors include beads, rings, pellets, extrudates, and flakes with size of millimeters.[2,3] However, these shaped catalysts not only retard the diffusion of guest molecules, decrease the selectivity of desirable products, suffer high-pressure drop brought by catalytic bed, and shorten the catalyst lifetime due to the quick coke deposition in high temperature but also result in the limited heat transfer rate, which make the process control difficult and influence the scale up of reactor.[4] Thus, a ZSM-5 structure with highly efficient diffusion channel and stable macroscopic structure, e.g., the well-organized meso-/macroporous structure, is highly desirable.[1d,5,6]

In recent years, structured catalysts, especially ZSM-5-coated monoliths, are reported to solve effectively part of these problems because of their improved diffusion rate, lower pressure drop, and avoidance of the use of binders for the final macroscopic shaping when compared to the shaped catalysts.[4b,7,8] However, the monoliths may not contain enough coating ZSM-5 for a given reactor volume to afford the desired catalytic performance, which limit their practical applications for many reacting systems.[9] In addition, the different thermal expansion coefficient between the support and the zeolites may result in the detachment of ZSM-5 layer from the supports under the frequent temperature shift and thus cause structure and operation failure.[7d,10]

To solve these problems, here, we propose an in situ fabrication method to prepare macroscopic *c*-axis oriented ZSM-5 hollow fibers with single crystal thickness (denoted as ZSM-5-CHF) using quartz fibers as the temporary soft substrate and Si source. The preparation of this unique structure involves two key steps. First, an efficient loading of silicalite seeds on the surface of quartz fibers is achieved by a low-speed centrifugation of the sample. Second, a direct solid−solid transformation method is applied to void the separation between the seeds and the substrates, thus leading to *c*-oriented intergrowth. The detailed synthesis procedure is better described in the Supporting Information (SI). The as-obtained fibers are composed of pure *c*-axis oriented ZSM-5 crystal with high crystallinity, good structural stability, and high surface area and exhibit the long micro-/meso-/macroporous structure. As a result, it exhibits excellent catalytic performance in a model reaction of methanol to gasoline (MTG). Catalyst lifetime of ZSM-5-CHF can be more than two-folds of that for conventional, randomly packed ZSM-5. This approach opens an alternative way to the pure zeolite-structured catalysts with improved mass and heat diffusion rate, lower pressure drop, and avoidance of the use of binders and also provides new insights for future development of adsorbents, separators, and microreactors.

The quartz fiber template has a smooth surface and solid structure with a diameter around 2−4 μm (Figure 1a and inset). The as-produced ZSM-5-CHF preserve the original morphology of quartz fibers, but their diameters double compared to pristine quartz fibers (Figure 1b). Average length of these ZSM-5 hollow fibers, observed under optical microscopy, is at least on the millimeter scale since their length is unable to be covered under optical microscopy even with the lowest magnification of 40 times (Figure S2c). Apparently, the in situ transformation method here just changes the diameter, not the length of the ZSM-5 fibers, which directly depends on that of quartz fibers (Figures S2a and S2b). The outer surface of ZSM-5 fibers is composed of densely packed submicrometer *c*-axis oriented ZSM-5 perpendicular to its

Received: August 20, 2013
Published: October 3, 2013

   dx.doi.org/10.1021/ja408624x | *J. Am. Chem. Soc.* 2013, 135, 15322−15325

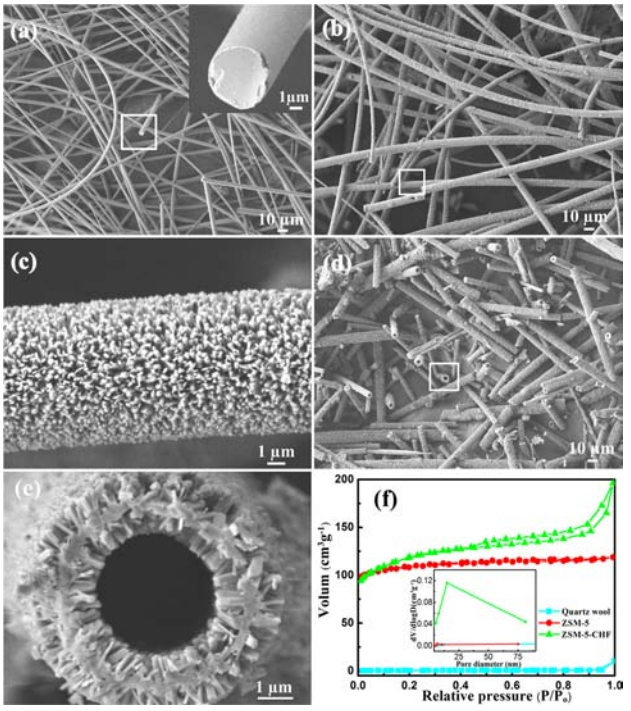

Figure 1. Low-magnification SEM images of (a) pristine quartz fibers; (b) ZSM-5-CHF; and (d) crushed ZSM-5-CHF. (c,e) High magnification SEM images of the part surrounded with a white frame in (b,d), respectively. (f) Nitrogen adsorption/desorption isotherms and BJH pore size distribution calculated from the adsorption branch of the isotherm (inset) for pristine quartz fibers, conventional ZSM-5, and ZSM-5-CHF.

surface (Figures 1c and S3a). Crushing some ZSM-5 fibers slightly reveals their hollow structure (Figure 1d), and the SEM image of the cross-section of a fiber indicates that dense ZSM-5 crystals grow inside and outside around a cylinder. They firmly bond by the middle cylinder with a growth direction perpendicular to the cylinder surface (Figure 1e). Obviously, the unique structured ZSM-5-CHF exhibits different pore structure from the conventional ZSM-5. Nitrogen adsorption/desorption isotherms of ZSM-5-CHF (Figure 1f) exhibit a typical adsorption curve of type I plus IV with an apparent enhanced uptake and an obvious hysteresis loop in the P/P_o range of 0.5−1,[11] indicating its remarkable micro-/meso-/macroporous structure. As a result, the BET surface area increases from 0.9 $m^2\ g^{-1}$ for the pristine quartz fibers to 409.8 $m^2\ g^{-1}$ for ZSM-5-CHF. In addition, ZSM-5-CHF possesses a broad pore distribution with a mean pore size of ∼18 nm (Figure 1f, inset), which belongs to the stacking pores of aggregated ZSM-5. Accordingly, the total pore volume increases from 0 to 0.31 $cm^3\ g^{-1}$, and mesopore volume increases from 0 to 0.16 $cm^3\ g^{-1}$. In addition, the mesopore volume of ZSM-5-CHF is also much higher than that for the conventional ZSM-5 (0.02 $cm^3\ g^{-1}$).

The structure of ZSM-5-CHF is intact after ultrasonic treatment for the sample preparation for TEM characterization (Figure 2a), indicating good mechanical stability due to the strong interaction of the inside or outside ZSM-5 crystals with the middle ZSM-5 cylinder (Figure 2a). Although the thickness of them in the *b*-axis is only 100−300 nm, the high density of *c*-axis oriented ZSM-5 crystals may ensure their structural stability (Figure 2b). TEM image (Figure 2a) shows that the contrast at the center is much lower than that of a solid fiber,

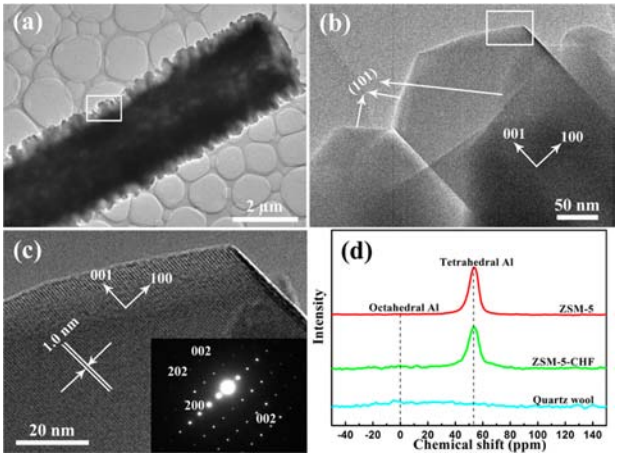

Figure 2. (a) TEM image of the ZSM-5-CHF. (b,c) HR-TEM images of the ZSM-5-CHF taken from the square frame in (a,b); the inset is its corresponding electron diffraction pattern. (d) ^{27}Al-NMR spectra of pristine quartz fibers, ZSM-5-CHF, and conventional ZSM-5.

further confirming the hollow structure. The ZSM-5-CHF are highly crystalline, with a lattice spacing of exactly 1.0 nm which is assigned to the (200) lattice plane of the ZSM-5 crystals (Figure 2c). The corresponding selected area electron diffraction (Figure 2c inset) shows the single ZSM-5 crystal nature when viewed down the [010] zone axis. In addition, analysis of ^{27}Al MAS NMR spectroscopy and ICP-OES is made to evidence the completed incorporation of aluminum atoms into the silica framework of ZSM-5-CHF, considering the catalytically active acid sites of aluminosilicate zeolites are generally correlated to the presence of intraframework aluminum atoms. The ^{27}Al MAS NMR spectrum (Figure 2d) of pristine quartz fibers shows no peak belongs to octahedral or tetrahedral Al. But only one sharp aluminum peak is at 52 ppm for the ZSM-5-CHF sample on the ^{27}Al MAS NMR spectrum (Figure 2d). It validates that all aluminum atoms are incorporated into the ZSM-5 framework with tetrahedral coordination environment.[12] ICP-OES analysis indicates that the Si/Al of ZSM-5-CHF is 95 (Table S1), which is close to the expected stoichiometry based on the composition of the seeded quartz fibers.

Note here that the in situ transformation does not change the macroscopic appearance of the quartz fiber aggregates (Figure 3Aa,Af). Their volume based on the same weight (0.75 g) is nearly the same and is strikingly larger than that of the conventional ZSM-5 (Figure 3Ag). The detailed transformation process of an individual quartz fiber into ZSM-5 hollow fiber at different times is shown in Figure 3B. As revealed by the characterization of a thin ZSM-5 cylinder with 200−300 nm in thickness, which is intentionally detached from the quartz fiber after the crystallization at 180 °C for 40 min (Figure S6), the initially grown ZSM-5 crystals have a coffin shape with a long *c*-axis and short *b*-axis (Lc > La > Lb), which is similar to the structure of silicate-1 synthesized with TPAOH (tetrapropylammonium hydroxide) as the template.[13] Such morphology makes the attachment of these ZSM-5 crystals on the quartz fiber surface with their *b*-axes perpendicular to the substrate surface to achieve the most stable state (Figure S6).[13] Although there are still many holes on the cylinder due to the short growth time, these spaces are then filled by the new-born ZSM-5 crystals, and the thin b-oriented ZSM-5 cylinders are developed into a thick and solid *b*-oriented cylinder after 1 h

dx.doi.org/10.1021/ja408624x | J. Am. Chem. Soc. 2013, 135, 15322−15325

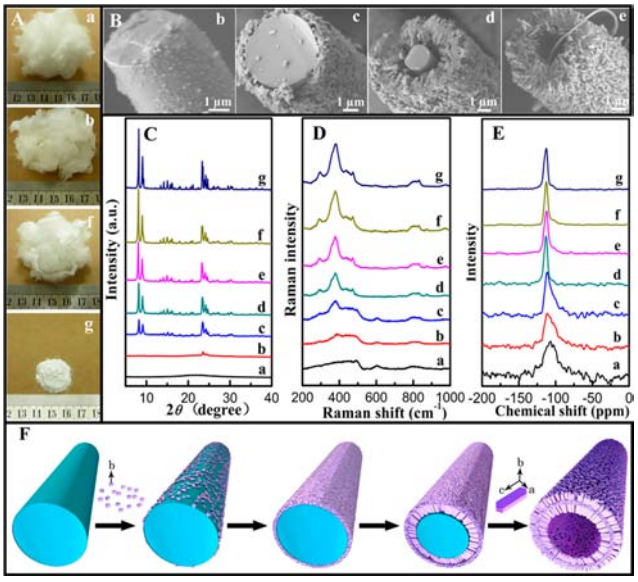

Figure 3. Investigation on ZSM-5-CHF crystallization. (A) Photographs, (B) SEM images, (C) XRD patterns, (D) UV-Raman spectra, (E) ^{29}Si NMR spectra of (a) the pristine quartz fibers, samples crystallized at (b) 0, (c) 1, (d) 1.5, (e) 2.2, and (f) 24 h for synthesizing ZSM-5-CHF, and (g) conventional ZSM-5 with the same weight as ZSM-5-CHF. (F) Schematic illustration of the growth mechanism of the ZSM-5-CHF.

crystallization time (Figure 3Bc). More interesting, upon further steam-assisted crystallization for 0.5 h, a layer of submicrometer ZSM-5 is first formed on the inside surface of this ZSM-5 cylinder with the *c*-axis perpendicular to the surface (Figure 3Bd). Actually, when the growth of *c*-axis oriented ZSM-5 inside cylinder is terminated due to space confinement inside and limitation of *c*/*b* ratio for an MFI-structured zeolite, the migration of Si species allows the continuous growth of *c*-axis oriented ZSM-5 outside the cylinder, until the whole quartz fibers are consumed (Figure 3Be). Detailed TEM images of the thick cylinder and the interacted part of cylinder with vertical *c*-axis oriented ZSM-5 crystal are unavailable due to technical limitation. The further growth of *c*-axis oriented ZSM-5 over the surface of *b*-oriented ZSM-5 cylinder is likely to follow an intergrowth mechanism dominantly, which is widely observed in the growth of ZSM-5,[14] and is closely related to the preferential growth of *c*-axis oriented crystal due to the quicker growth rate along *c*-axis direction under the sufficient supply of Si source from the quartz fibers.[13] Figure 3C–E shows XRD patterns, UV-Raman spectra, and ^{29}Si NMR spectra of the samples crystallized at various times, respectively. The pristine quartz fibers have an XRD pattern consistent with amorphous silica. After seeding, the sample exhibits an extremely faint XRD pattern of MFI structure.[6b,15] As crystallization continued, the intensity of the characteristic MFI-structured peaks increases rapidly and draws near the maximum after 2.2 h treatment. The completed conversion of quartz fibers to ZSM-5 crystals within just a few hours suggests that the presence of seeds plays an important role in shortening the nucleation stage, which is always the most time-consuming step in preparing ZSM-5. The peak intensity of the sample after 24h crystallization in XRD pattern was comparable to that of conventional ZSM-5, demonstrating the high crystallinity of ZSM-5-CHF. Similar trends are also observed for UV-Raman and ^{29}Si NMR spectra. Compared with amorphous quartz fibers, the UV-Raman spectra of the samples after crystallization show a wide band at 380 cm^{-1} (Figure 3D) associated with the framework symmetric stretching vibration of a five-membered building unit in MFI-type zeolites.[16] After the treatment at 180 °C for 1.5 h, the ^{29}Si NMR spectrum of the sample (Figure 3E) emerges a sharp peak at −112 ppm and a shoulder at −105 ppm, demonstrating a significant condensation of silica species. The strong peak can be assigned to Si(0Al) contribution and the shoulder peak to the Si(1Al) contribution, which also indicates the successful incorporation of aluminum atoms into the ZSM-5-CHF framework.[17] According to the study of the evolution process, the formation mechanism of ZSM-5-CHF is described by schematic illustrations as shown in Figure 3F.

It is well-known that the use of hollow fiber geometry has long been an effective solution to improve the performance of membrane-based separation processes.[18] However, the incorporation of aluminum atoms into the framework of silicalite-1 would reduce its hydrophobicity leading to worse selective separation properties.[18b] So, here, *c*-axis oriented silicalite-1 hollow fibers (denoted as silicalite-1-CHF, Figure S7) with a similar structure as ZSM-5-CHF are also prepared under the same synthetic process except the adding of Al source (SI). The SEM images, XRD patterns, and nitrogen adsorption/desorption isotherms (Figures S7–S9) demonstrate the high-crystalline MFI structure and well-ordered *c*-axis oriented feature of the silicalite-1-CHF, which give them very promising applications for adsorption, separation with high selectivity, stability, and durability.

It is expected that the hollow and 1D order structure with abundant intercrystalline voids could offer high surface-to-volume (*S*/*V*) ratio for ZSM-5-CHF. This feature may effectively enhance the mass and heat transfer of guest molecules and also the utilization of catalyst. Hence, in order to test its catalytic performance, MTG reaction is carried out over ZSM-5-CHF and conventional ZSM-5 in a fixed bed stainless steel reactor (reaction temperature: 673 K, WHSV: 8 h^{-1}). Under high space velocity, both the ZSM-5-CHF and the conventional ZSM-5 show similar initial methanol conversions of around 87% (Figure 4). However, with time on stream, the

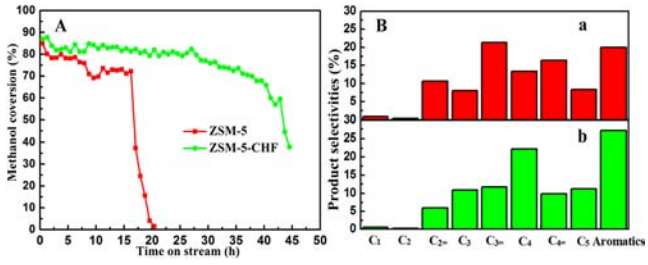

Figure 4. (A) Methanol conversions over conventional ZSM-5 and ZSM-5-CHF as a function of time on stream (reaction temperature: 673 K, WHSV: 8 h^{-1}). (B) Product selectivity of MTG reactions over the conventional ZSM-5 (a) and the ZSM-5-CHF (b) after 2 h time on stream.

ZSM-5-CHF is deactivated far slower than the conventional ZSM-5. Since the acid strength and amount, Si/Al ratio, and micropore volume are similar for conventional ZSM-5 and ZSM-5-CHF (Figures S4 and S5, Table S1), the excellent catalytic stability over the ZSM-5-CHF can be directly attributed to the unique structure of the ZSM-5-CHF which favors the evacuation of the coke precursors and reduces the coking reaction rate especially for the strongly exothermic

dx.doi.org/10.1021/ja408624x | J. Am. Chem. Soc. 2013, 135, 15322–15325

MTG reaction.[19] Actually, TG profiles (Figure S10) show the used ZSM-5-CHF has a coke formation rate of 1.2 mg g_{cat}^{-1} h^{-1}, much lower than that of 4.3 mg g_{cat}^{-1} h^{-1} observed over used conventional ZSM-5. The selectivity of product at 2 h on stream is also given in Figure 4B. The ZSM-5-CHF exhibits higher selectivity of producing aromatics and C_5 paraffin compared with conventional ZSM-5. Quantitatively, the selectivity of C_{5+} over ZSM-5-CHF, belonging to the gasoline cut,[20] is up to 39%, far higher (28%) than conventional ZSM-5. These results show the meso-/macroporous hollow structure of ZSM-5-CHF is very effective in increasing the product selectivity and catalytic efficiency.

In summary, we successfully synthesize *c*-axis oriented ZSM-5 hollow fibers (ZSM-5-CHF) using quartz fibers as the silica source and the temporary soft substrate based on an in situ solid−solid transformation mechanism. The growth of such unique structure undergoes the developing of *b*-oriented ZSM-5 cylinder on quartz fibers, followed by the growth of *c*-axis oriented ZSM-5 crystal inside and finally outside the cylinder. The obtained sample exhibits high crystallinity, good structural stability, high surface area, and superior catalytic performance for MTG reaction, demonstrating great potential as an industrial catalyst. Furthermore, the implementation of crystal shape engineering based on an in situ solid−solid transformation mechanism should be easily extended to synthesize other zeolites and also provides new insights for future development of adsorbents, separators, and microreactors.

■ ASSOCIATED CONTENT

Supporting Information

Synthesis and characterization details. This material is available free of charge via the Internet at http://pubs.acs.org.

■ AUTHOR INFORMATION

Corresponding Author

qianwz@ tsinghua.edu.cn

Notes

The authors declare no competing financial interest.

■ ACKNOWLEDGMENTS

The authors thank the support of NSFC program of 21376135 and NSFC key program of 51236004.

■ REFERENCES

(1) (a) Corma, A. *Chem. Rev.* **1997**, *97*, 2373. (b) Cundy, C. S.; Cox, P. A. *Chem. Rev.* **2003**, *103*, 663. (c) Roeffaers, M. B.; Ameloot, R.; Baruah, M.; Uji-i, H.; Bulut, M.; De Cremer, G.; Müller, U.; Jacobs, P. A.; Hofkens, J.; Sels, B. F. *J. Am. Chem. Soc.* **2008**, *130*, 5763. (d) Shen, K.; Qian, W.; Wang, N.; Zhang, J.; Wei, F. *J. Mater. Chem. A* **2013**, *1*, 3272.

(2) (a) Degnan, T.; Chitnis, G.; Schipper, P. *Microporous Mesoporous Mater.* **2000**, *35*, 245. (b) Yang, G.; He, J.; Yoneyama, Y.; Tan, Y.; Han, Y.; Tsubaki, N. *Appl. Catal., A* **2007**, *329*, 99. (c) Keil, F. J.; Hinderer, J.; Garayhi, A. R. *Catal. Today* **1999**, *50*, 637.

(3) (a) Lee, Y.-J.; Kim, Y.-W.; Viswanadham, N.; Jun, K.-W.; Bae, J. W. *Appl. Catal., A* **2010**, *374*, 18. (b) Chen, D.; Wang, J.; Ren, X.; Teng, H.; Gu, H. *Catal. Lett.* **2010**, *136*, 65. (c) Yuranov, I.; Bulushev, D. A.; Renken, A.; Kiwi-Minsker, L. *J. Catal.* **2004**, *227*, 138.

(4) (a) Richardson, J.; Peng, Y.; Remue, D. *Appl. Catal., A* **2000**, *204*, 19. (b) Zampieri, A.; Colombo, P.; Mabande, G. T.; Selvam, T.; Schwieger, W.; Scheffler, F. *Adv. Mater.* **2004**, *16*, 819. (c) Dong, A.; Wang, Y.; Tang, Y.; Ren, N.; Zhang, Y.; Yue, Y.; Gao, Z. *Adv. Mater.* **2002**, *14*, 926.

(5) (a) Kim, J.; Choi, M.; Ryoo, R. *J. Catal.* **2010**, *269*, 219. (b) Choi, M.; Cho, H. S.; Srivastava, R.; Venkatesan, C.; Choi, D.-H.; Ryoo, R. *Nat. Mater.* **2006**, *5*, 718. (c) Choi, M.; Na, K.; Kim, J.; Sakamoto, Y.; Terasaki, O.; Ryoo, R. *Nature* **2009**, *461*, 246. (d) Na, K.; Jo, C.; Kim, J.; Cho, K.; Jung, J.; Seo, Y.; Messinger, R. J.; Chmelka, B. F.; Ryoo, R. *Science* **2011**, *333*, 328. (e) Shetti, V. N.; Kim, J.; Srivastava, R.; Choi, M.; Ryoo, R. *J. Catal.* **2008**, *254*, 296.

(6) (a) Liu, F.; Willhammar, T.; Wang, L.; Zhu, L.; Sun, Q.; Meng, X.; Carrillo-Cabrera, W.; Zou, X.; Xiao, F.-S. *J. Am. Chem. Soc.* **2012**, *134*, 4557. (b) Ren, L.; Wu, Q.; Yang, C.; Zhu, L.; Li, C.; Zhang, P.; Zhang, H.; Meng, X.; Xiao, F.-S. *J. Am. Chem. Soc.* **2012**, *134*, 15173.

(7) (a) Shan, Z.; Van Kooten, W.; Oudshoorn, O.; Jansen, J.; Van Bekkum, H.; Van Den Bleek, C.; Calis, H. *Microporous Mesoporous Mater.* **2000**, *34*, 81. (b) Trong, On, D.; Kaliaguine, S. *J. Am. Chem. Soc.* **2003**, *125*, 618. (c) Liu, Y.-M.; Feng, W.-L.; Li, T.-C.; He, H.-Y.; Dai, W.-L.; Huang, W.; Cao, Y.; Fan, K.-N. *J. Catal.* **2006**, *239*, 125. (d) Ivanova, S.; Louis, B.; Madani, B.; Tessonnier, J.; Ledoux, M.; Pham-Huu, C. *J. Phys. Chem. C* **2007**, *111*, 4368.

(8) (a) Perez-Ramirez, J.; Christensen, C. H.; Egeblad, K.; Christensen, C. H.; Groen, J. C. *Chem. Soc. Rev.* **2008**, *37*, 2530. (b) Louis, B.; Ocampo, F.; Yun, H.; Tessonnier, J.; Pereira, M. M. *Chem. Eng. J.* **2010**, *161*, 397. (c) Chen, H.; Zhang, H.; Yan, Y. *Ind. Eng. Chem. Res.* **2012**, *51*, 16643. (d) Jiao, Y.; Jiang, C.; Yang, Z.; Zhang, J. *Microporous Mesoporous Mater.* **2012**, *162*, 152.

(9) (a) Buciuman, F.-C.; Kraushaar-Czarnetzki, B. *Catal. Today* **2001**, *69*, 337. (b) Kiwi-Minsker, L.; Renken, A. *Catal. Today* **2005**, *110*, 2.

(10) Louis, B.; Tezel, C.; Kiwi-Minsker, L.; Renken, A. *Catal. Today* **2001**, *69*, 365.

(11) (a) Imperor-Clerc, M.; Davidson, P.; Davidson, A. *J. Am. Chem. Soc.* **2000**, *122*, 11925. (b) Trong, On, D.; Kaliaguine, S. *Angew. Chem.* **2001**, *113*, 3348. (c) Liu, X.; Tian, B.; Yu, C.; Gao, F.; Xie, S.; Tu, B.; Che, R.; Peng, L. M.; Zhao, D. *Angew. Chem., Int. Ed.* **2002**, *41*, 3876.

(12) (a) Do, T.-O.; Nossov, A.; Springuel-Huet, M.-A.; Schneider, C.; Bretherton, J. L.; Fyfe, C. A.; Kaliaguine, S. *J. Am. Chem. Soc.* **2004**, *126*, 14324. (b) Dědeček, J. i.; Sklenak, S.; Li, C.; Wichterlová, B.; Gábová, V.; Brus, J. i.; Sierka, M.; Sauer, J. *J. Phys. Chem. C* **2009**, *113*, 1447.

(13) (a) Lai, Z.; Bonilla, G.; Diaz, I.; Nery, J. G.; Sujaoti, K.; Amat, M. A.; Kokkoli, E.; Terasaki, O.; Thompson, R. W.; Tsapatsis, M. *Science* **2003**, *300*, 456. (b) Lai, Z.; Tsapatsis, M.; Nicolich, J. P. *Adv. Funct. Mater.* **2004**, *14*, 716.

(14) (a) Hay, D.; Jaeger, H.; Wilshier, K. *Zeolites* **1990**, *10*, 571. (b) Weidenthaler, C.; Fischer, R.; Shannon, R.; Medenbach, O. *J. Phys. Chem.* **1994**, *98*, 12687. (c) Wang, Z.; Hedlund, J.; Zhang, H.; Zou, X. *Microporous Mesoporous Mater.* **2006**, *95*, 86.

(15) Wu, E.; Lawton, S.; Olson, D.; Rohrman, A.; Kokotailo, G. *J. Phys. Chem.* **1979**, *83*, 2777.

(16) (a) Dutta, P. K.; Puri, M. *J. Phys. Chem.* **1987**, *91*, 4329. (b) Dutta, P. K.; Rao, K. M.; Park, J. Y. *J. Phys. Chem.* **1991**, *95*, 6654.

(17) Fyfe, C.; Gobbi, G.; Kennedy, G.; Graham, J.; Ozubko, R.; Murphy, W.; Bothner-By, A.; Dadok, J.; Chesnick, A. *Zeolites* **1985**, *5*, 179.

(18) (a) Alshebani, A.; Pera-Titus, M.; Landrivon, E.; Schiestel, T.; Miachon, S.; Dalmon, J.-A. *Microporous Mesoporous Mater.* **2008**, *115*, 197. (b) Shan, L.; Shao, J.; Wang, Z.; Yan, Y. *J. Membr. Sci.* **2011**, *378*, 319.

(19) Antia, J. E.; Govind, R. *Ind. Eng. Chem. Res.* **1995**, *34*, 140.

(20) Bjørgen, M.; Joensen, F.; Spangsberg Holm, M.; Olsbye, U.; Lillerud, K.-P.; Svelle, S. *Appl. Catal., A* **2008**, *345*, 43.